An EPR/ENDOR and Computational Study of Outer Sphere Interactions in Copper Complexes of Phenolic Oximes

*Mary R. Healy,[1] Emma Carter,[2] Ian A. Fallis,[2] Ross S. Forgan,[1] Ross J. Gordon,[1] Eduardo Kamenetzky,[3] Jason B. Love,[1] Carole A. Morrison,[1] *Damien M. Murphy,[2] *Peter A Tasker[1].*

[1]EaStCHEM School of Chemistry, University of Edinburgh, Edinburgh, EH9 EJJ, UK.

[2]School of Chemistry, Cardiff University, Park Place, Cardiff, CF10 3AT, UK.

[3]Cytec Industries, 1937 West Main St, Stamford, CT, 06904-0060, USA

KEYWORDS

Electron Paramagnetic Resonance, Electron Nuclear DOuble Resonance, Oximes, Copper, Solvent Extraction.

ABSTRACT

Copper complexes of the phenolic oxime family of ligands (3-*X*-salicylaldoximes) are used extensively as metal solvent extractants. Incorporation of electronegative substituents in the 3-position, *ortho* to the phenol group, can be used to "buttress" the inter-ligand H-bonding leading to enhancement in extractant strength. However, investigation of the relevant H-bonding in these complexes can be exceedingly difficult. Here we have combined EPR, ENDOR, DFT and X-ray crystallography to study this effect. Analysis of the ^{1}H ENDOR data revealed a variation in the Cu…H^{16} (oxime proton) distance from 2.92 Å for the unsubstituted complex [Cu($\mathbf{L}^{2}$)$_2$] compared to 3.65 Å for the *X* = N(C_6H_{13})$_2$ substituted complex [Cu($\mathbf{L}^{3}$)$_2$]. DFT calculations showed that this variation is caused by changes to the length and strength of the H-bond between the oximic hydrogen and the phenolate oxygen. Noticeable changes to the Cu…H^{15} (azomethine proton) distances and the Cu…N bonding were also observed in the two complexes, as revealed through the ^{N}A and ^{N}Q ENDOR data. Distortions in the structure of the complex and variations in the oximic proton to phenolate oxygen H-bond strength caused by the substituent (*X*) were confirmed by DFT and X-ray crystallography. DFT directly evidenced the importance of the interaction between H^{16} and the amine nitrogen of N(C_6H_{13})$_2$ in the buttressed complex, and how the high strength of this interaction may not necessarily lead to enhancement of copper extraction as it can impose an unfavorable geometry in the inner coordination sphere of the complex. Therefore ENDOR, DFT and X-ray structural data all indicate that the aminomethyl substituent (X) *ortho* to the phenolic oxygen atom provides a particularly strong buttressing of inter-ligand H-bonding in these copper complexes, and these outer sphere interactions can significantly influence structure and stability.

Introduction

The interaction between ligands in the outer coordination spheres of metal ions often contributes to the thermodynamic and kinetic stability of the complexes in systems as diverse as antibiotics,[1] gravimetric reagents[2] and metal solvent extractants.[3a,b] The last are used in kilotonne-scale processes in extractive metallurgy and provide very efficient ways to achieve the necessary operations for concentration and separation of metals dissolved in aqueous acidic solution by selective phase transfer into an organic phase.[4] The hydrogen bonding (H-bonding) interactions of metal complexes[5] and in particular between ligands is particularly favored in the high boiling non-polar solvents used by industry for metal solvent extraction and is often responsible for the selectivity of extraction which is essential for efficient recovery processes. Metal extraction by organic derivatives of phosphorus(V) acids, such as the commercial used reagent *di*-(2-ethylhexyl)phosphoric acid (D2EHPA), is usually associated with retention of strong inter-ligand H-bonds and the formation of 8-membered pseudo-chelate rings (Scheme 1a)[4b], favoring complex formation with tetrahedral metal cations leading to selectivity for Zn(II) over other 1st row transition metal (II) cations. This selectivity is now exploited in a zinc-plant in Namibia which operates on a 150,000 tonne per annum scale.[6]

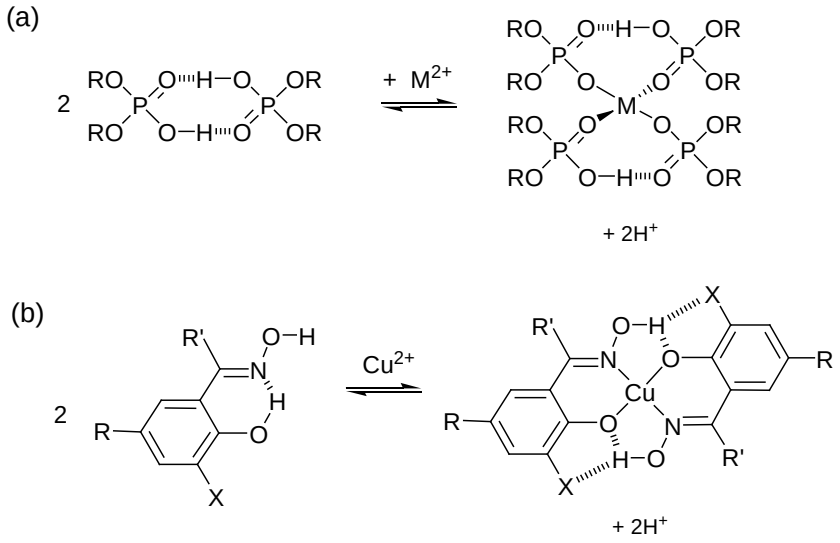

Scheme 1. Two "pH-swing" extractants which form inter-ligand H-bonds: a) the phosphoric acid diesters (*e.g.*, D2EHPA, R = 2-ethylhexyl) which is used in zinc recovery,[6] and b) the 5-alkyl-substituted salicylaldoximes (R′ = X = H) used in copper recovery.[7]

Inter-ligand H-bonding is also important in determining the extraction strength and selectivity of the phenolic oxime reagents (Scheme 1b) used in copper recovery[7] which now account for between 20 and 30% of the world's production of copper.[8] The incorporation of electronegative substituents (X) in the 3-position, *ortho* to the phenol group (Scheme 1b) can be used to "buttress" the inter-ligand H-bonding and leads to substantial increases in extractant strength.[9]

Structural information on copper complexes of the phenolic oximes in the regions which form the inter-ligand H-bonds is important in understanding the origins of such buttressing effects but is difficult to obtain. The precision with which H-atoms can be located in transition metal complexes by X-ray structure determination is limited, and, in the solid state, Cu-cations have a propensity to form weak bonds to donor atoms in neighboring molecules which in turn influences the Cu-O and Cu-N bond lengths in the cavity of the molecule and changes the inter-ligand contact distances.[10] In order to replicate the conditions which apply in solvent extraction,

it is preferable to probe the structures of the complexes in solution. Fortunately, the paramagnetism of Cu(II) enables the systems to be readily characterized using advanced EPR techniques and therefore in this paper we have utilized a combination of continuous wave (CW) Electron Paramagnetic Resonance (EPR) and Electron Nuclear DOuble Resonance (ENDOR) spectroscopy, supported by computational methods, to determine the variation in Cu…^{1}H distances as a function of changes in the outer coordination sphere of some of the compounds shown in Scheme 2. The predicted strengths of the hydrogen bonds and differences in the copper coordination spheres are discussed within the context of experimental structures, solvent extractions and X-ray structures.

Experimental Section

The syntheses of the proligands $\mathbf{L^{2}}$H, $\mathbf{L^{3}}$H, $\mathbf{L^{6}}$H, $\mathbf{L^{9}}$H and $\mathbf{L^{10}}$H (scheme 2) and the associated preparation and characterization, including X-ray structure determinations of their copper complexes have been reported previously.[9,11]

EPR/ENDOR Spectroscopy: X-band (9 GHz) CW-EPR spectra were recorded at 140 K on a Bruker EMX spectrometer operating at 100 kHz field modulation, 10 mW microwave power using an ER 4119HS cavity. Q-band (35 GHz) CW-EPR and ENDOR spectra were recorded on a Bruker ESP 300E series spectrometer equipped with an ESP360 DICE ENDOR unit operating at 12.5 kHz field modulation in a Q-band ENDOR cavity (Bruker ER 5106 QT-E). The ENDOR spectra were obtained using 8 dB RF power from an ENI A-300 RF amplifier and 50 or 200 kHz RF modulation depth and 1 mW microwave power. Q-band EPR spectra were recorded at 50 K,

while the Q-band ENDOR measurements were performed at 10 K. Spectral simulations were performed using the EasySpin toolbox in Matlab developed at ETH Zurich.[12]

Computations: All calculations were executed using the Gaussian '09 program.[13] Full structural optimizations and NBO06[14] analyses were carried out using the hybrid DFT functional B3LYP,[15] coupled to the 6-31+G(d,p) basis set for each of the proligands, proligand dimers and copper complexes. Vibrational frequency calculations were carried out on all optimized structures to ensure energy minima had been reached. Assembly formation energies, dimerization and deprotonation energies were calculated using the difference in internal energy values based on the sum of the products and the sum of individual reactants. A correction factor for basis set superposition error (BSSE) was also included which was determined using the counterpoise method of Boys and Bernardi.[16]

Results and Discussion

$\mathbf{L^1}$H represents the unsubstituted proligand. The [Cu($\mathbf{L^1}$)$_2$] complex was studied several years ago using ENDOR spectroscopy by Schweiger as a doped single crystal and solid solution using the isomorphous [Ni($\mathbf{L^1}$)$_2$] complex.[17,18,19] The *t*-butyl and *n*-hexyl groups in $\mathbf{L^2}$H and $\mathbf{L^3}$H provide sufficient solubility in non-polar solvents to allow extraction experiments to be carried out and for these solutions to be subsequently characterized by EPR and ENDOR spectroscopy. Methyl substituents were used in the DFT calculations (labeled $\mathbf{L^4}$H, $\mathbf{L^5}$H, $\mathbf{L^7}$H, $\mathbf{L^8}$H; see below) to reduce the number of conformers in the side chains when defining energy-minimized forms, whilst the restricted flexibility of the piperidine group in $\mathbf{L^6}$H permitted the isolation of single crystals of [Cu($\mathbf{L^6}$)$_2$] suitable for X-ray structure determination.[11] It is worth nothing that commercial extractants normally carry branched mixed isomer nonyl or dodecyl groups in the 5-

position to impart solubility in kerosene organic phases. The EPR spectra of copper complexes bearing such commercial extractants have been reported previously, providing evidence that 2:1 complexes of the type shown in Scheme 2 are formed in hydrocarbon solvents and that adducts can be formed with strongly basic ligands such as ammonia or pyridine.[20]

	R	X
L^1H	H	H
L^2H	*t*-Bu	H
L^3H	*t*-Bu	$(n_6\text{-}C_6H_{13})_2NCH_2$
L^4H	Me	H
L^5H	Me	Me_2NCH_2
L^6H	*t*-Bu	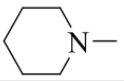
L^7H	Me	Br
L^8H	Me	*t*-Bu
L^9H	*t*-Bu	Br
$L^{10}H$	*t*-Bu	*t*-Bu

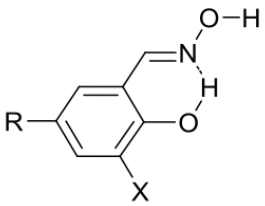

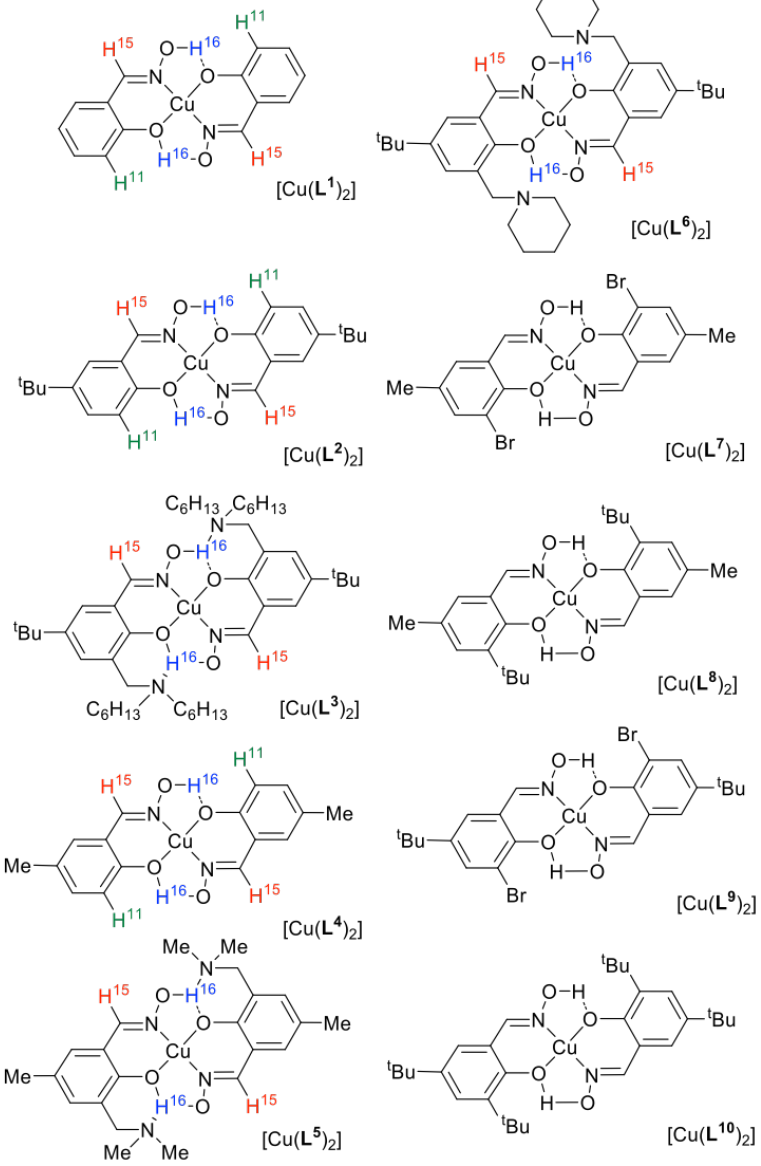

Scheme 2. Structures of the complexes and the labeling used to define the hydrogen atoms in the azomethine (H^{15}) and oxime (H^{16}) groups and in the 3-phenyl position (H^{11}) of [Cu(**L^1**)$_2$].

X- and Q-band EPR

Low temperature (140 or 50 K) CW EPR measurements of [Cu($\mathbf{L}^2$)$_2$] and [Cu($\mathbf{L}^3$)$_2$] were undertaken at both X- and Q-band frequencies and the resulting spectra are shown in Figures 1 (9 GHz) and ESI 1 (35 GHz). The well resolved X-band EPR spectra contain a large number of lines arising from the superhyperfine interactions to neighboring ligand nuclei (^{14}N, ^{1}H) and the spectra are further complicated by the presence of additional features arising from angular anomalies. These anomalies occur because, to first order, the hyperfine splittings remain equal at any orientation;[21,22] the relative anisotropy of $\boldsymbol{g}$ and $^{Cu}\boldsymbol{A}$ in any plane will then determine whether additional turning directions will occur for orientations away from the principal or canonical directions. The effects are usually observed in Cu(II) systems with relatively large anisotropy in the principal $\boldsymbol{g}$ values, combined with substantial hyperfine splittings in the perpendicular region of the spectrum, but they can be easily resolved by measurements at higher frequencies.

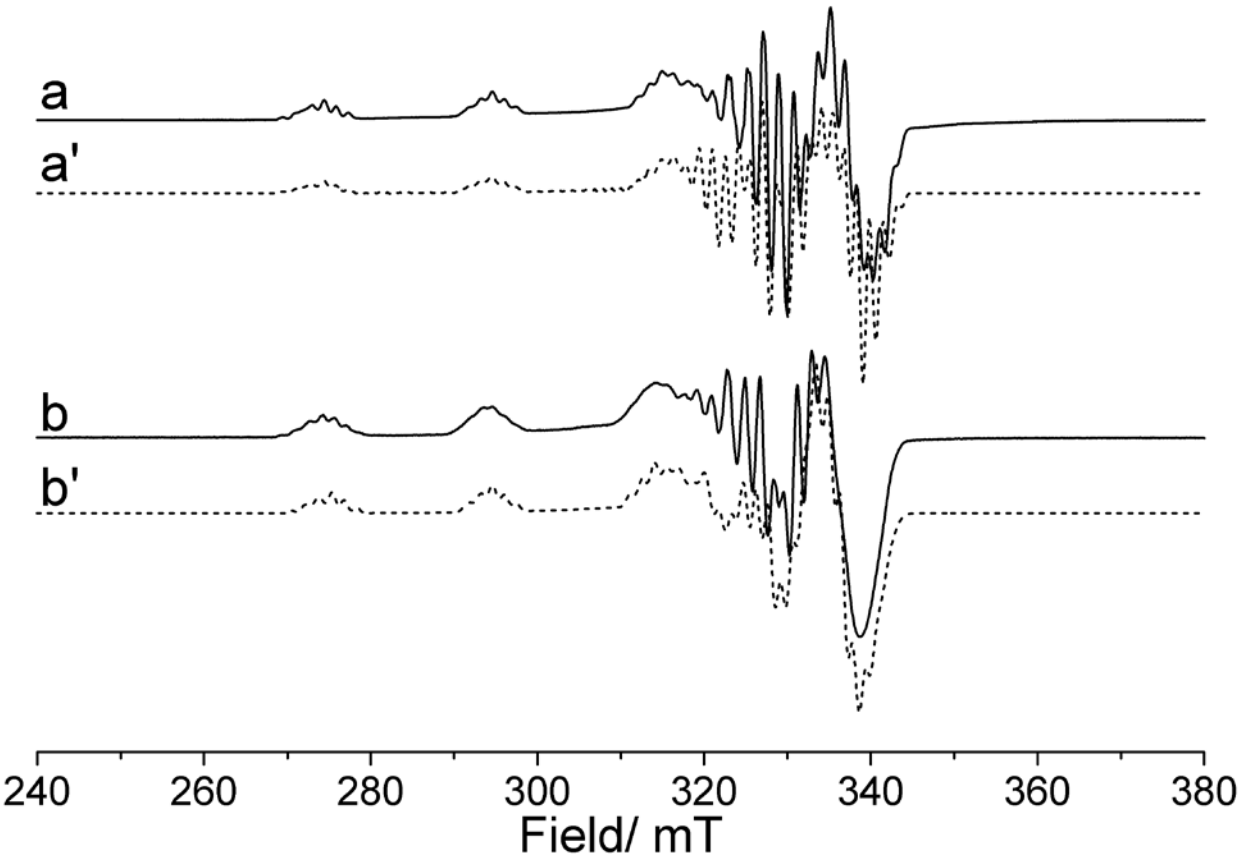

Figure 1. X-band CW EPR spectra (140 K) of: a) [Cu($\mathbf{L}^2$)$_2$] and b) [Cu($\mathbf{L}^3$)$_2$]. The corresponding simulations are shown in a′ and b′.

A solid state EPR and ENDOR investigation of the closely related [Cu($\mathbf{L}^1$)$_2$] complex (Scheme 2) was previously reported by Schweiger.[17,18,19] The principal values of the ***g*** and ^{Cu}***A*** tensors for the solid state [Cu($\mathbf{L}^1$)$_2$] are given in Table 1, where a slight rhombic distortion in ***g*** can be noted. These reported ***g/A*** values were used as a starting point to simulate the frozen solution X- and Q-band EPR spectra of [Cu($\mathbf{L}^2$)$_2$] and [Cu($\mathbf{L}^3$)$_2$] (Figure 1 and ESI 1). The agreement between the single crystal/solid solution data for [Cu($\mathbf{L}^1$)$_2$][17,18,19] and the frozen solution data presented here is excellent; a small difference is noted in the A_z ($A_{||}$) component of the ^{63,65}Cu hyperfine splitting and this is likely due to the solvent environment in [Cu($\mathbf{L}^2$)$_2$] and [Cu($\mathbf{L}^3$)$_2$] compared to the solid state [Ni($\mathbf{L}^1$)$_2$] matrix.[17,18,19] The spin Hamiltonian parameters are entirely consistent with a

system possessing a square planar geometry with a $d_{x^2-y^2}$ ground state.[23] Interestingly, the A_z ($A_{\|}$) splitting of [Cu($\mathbf{L^3}$)$_2$] (620 MHz) is smaller compared to [Cu($\mathbf{L^2}$)$_2$] (640 MHz) indicating that the influence of the outer sphere hydrogen bond accepting -N(C_6H_{13})$_2$ group can is observable in the EPR spectrum.

Table 1. ***g*** and ^{Cu}***A*** spin Hamiltonian parameters for [Cu($\mathbf{L^1}$)$_2$], [Cu($\mathbf{L^2}$)$_2$] and [Cu($\mathbf{L^3}$)$_2$]. The [Cu($\mathbf{L^2}$)$_2$] and [Cu($\mathbf{L^3}$)$_2$] samples were dissolved in a 1:1 toluene:dichloromethane mixture.

	$^{a}g_x$	$^{a}g_y$	$^{b}g_z$	$^{c}A_x$	$^{c}A_y$	$^{d}A_z$	Ref
[Cu($\mathbf{L^1}$)$_2$]	2.056	2.039	2.203	-109	-111	-609	17
[Cu($\mathbf{L^2}$)$_2$]	2.056	2.039	2.20	-109	-111	-640	*this work*
[Cu($\mathbf{L^3}$)$_2$]	2.050	2.039	2.20	-109	-111	-620	*this work*

All A_i values reported in MHz; [a] ±0.003, [b] ±0.003, [c] ±5, [d] ±3;

Q-band ^{1}H ENDOR

The CW ^{1}H ENDOR spectra, recorded at Q-band frequency for both [Cu($\mathbf{L^2}$)$_2$] and [Cu($\mathbf{L^3}$)$_2$], are shown in Figure 2 and ESI 2, respectively. The spectra were recorded over a range of magnetic field positions, ranging from 1080.0 mT to 1200.0 mT. This field range is necessary in order to extract the correct form of the ^{1}H tensor for an interacting ligand nucleus in the orientation selective ENDOR experiment.[24-27] Improved resolution of the ^{1}H resonances was obtained at Q-band frequencies, since the large azomethine couplings (see below) were overlapped with the strongly coupled ^{14}N signals in the X-band ENDOR spectra.

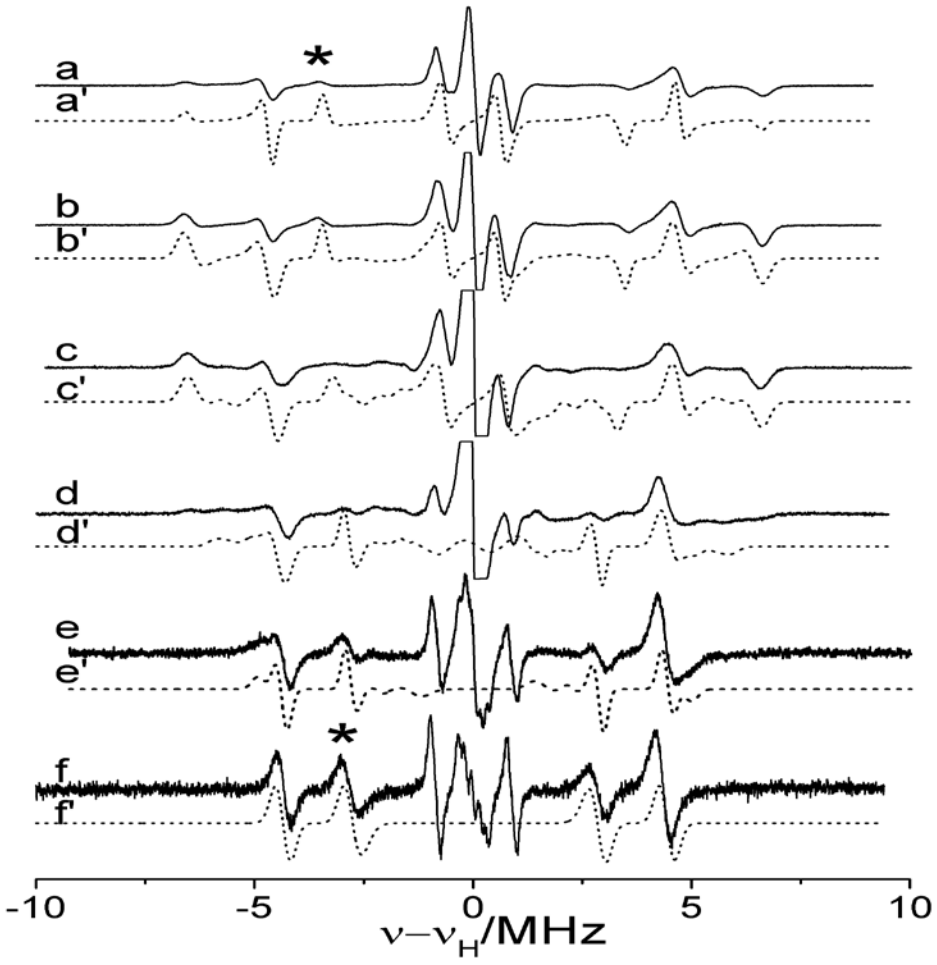

Figure 2: Q-band ^{1}H ENDOR spectra (10K) for [Cu(**L**^{2})$_2$] recorded at the field positions of a) 1200.1, b) 1195.5, c) 1181.8, d) 1144.1, e) 1102.9 and f) 1082.4 mT. Two peaks arising from the oxime proton (H^{16}) are marked with an asterix (the remaining A_2 component of this hyperfine is unresolved). Corresponding simulations are shown at each field position with dotted lines, labelled a′ – f′.

The ^{1}H ENDOR spectra are dominated by hyperfine couplings from two strongly coupled protons; namely the azomethine proton (labeled H^{15}) and the H-bonded oxime proton (labeled H^{16}), as shown in Scheme 2. These protons were also clearly distinguished in the single crystal

ENDOR study of [Cu($\mathbf{L^1}$)$_2$],[17] where they were labelled H^{15} and H^{16} respectively; for consistency we have adopted the same labeling of these protons. The corresponding simulations for the two proton couplings are shown in Figure 2 (and ESI 2) and the resulting principal values of the hyperfine tensors are listed in Table 2. Analysis of the data reveals that the azomethine protons (H^{15}) are dominated by a large isotropic hyperfine coupling of a_{iso} = 10.42 MHz in [Cu($\mathbf{L^2}$)$_2$] and a_{iso} = 10.23 MHz in [Cu($\mathbf{L^3}$)$_2$]. The lower a_{iso} value in [Cu($\mathbf{L^3}$)$_2$] simply indicates a smaller unpaired spin density on H^{15}.

In addition to these small differences in a_{iso}, the dipolar components of the ^{1}H hyperfine tensors ($^HA_{||}$) were also found to be different; *i.e.*, 2.78 MHz versus 2.47 MHz for [Cu($\mathbf{L^2}$)$_2$] and [Cu($\mathbf{L^3}$)$_2$] respectively. These $^HA_{||}$ values can be analyzed using a simple point-dipole approximation[28] to yield the resulting Cu…H^{15} distances of 3.97 Å and 4.13 Å respectively. This indicates that the X = -N(C_6H_{13})$_2$ group in [Cu($\mathbf{L^3}$)$_2$] influences the structural properties of the complexes, in this case by altering both the Cu…H^{15} distance and changing the Fermi contact term (a_{iso}). It is important to note that the hyperfine tensor for this H^{15} azomethine proton in [Cu($\mathbf{L^2}$)$_2$] is similar to that reported for [Cu($\mathbf{L^1}$)$_2$], confirming that the small changes reported in Table 2 by modification of the ligand in [Cu($\mathbf{L^3}$)$_2$] are real and meaningful.

Table 2; ^{1}H principal hyperfine values for [Cu($\mathbf{L^1}$)$_2$], [Cu($\mathbf{L^2}$)$_2$] and [Cu($\mathbf{L^3}$)$_2$].

	$^{a}A_1$	$^{b}A_2$	$^{a}A_3$	α	β	γ	a_{iso}	A_{dip}	R/ Å	Ref
[Cu($\mathbf{L^1}$)$_2$]$_{sc}$										
H^{15}	13.0	9.15	8.48	3.1499	0.0268	-2.746	10.21	2.79	3.97	17
H^{16}	6.60	-0.87	-5.97	1.771	0.0551	-2.5004	-0.08	6.68	2.94	17
[Cu($\mathbf{L^2}$)$_2$]$_{ply}$										
H^{15}	13.2	9.35	8.7	3.1499	0.0268	-2.746	10.42	2.78	3.97	*This work*
H^{16}	6.90	-1.25	-5.87	1.771	0.0551	-2.5004	-0.07	6.97	2.92	*This work*
[Cu($\mathbf{L^3}$)$_2$]$_{ply}$										
H^{15}	12.7	9.3	8.7	3.1499	0.0268	-2.746	10.23	2.47	4.13	*This work*
H^{16}	6.90	-1.25	-4.0	1.771	0.0551	-2.5004	0.55	3.65	3.01	*This work*

sc = Single crystal data; ply = polycrystalline toluene/dichloromethane frozen solution;

α ,β, γ = Euler angles. All hyperfine values are reported in MHz; a ± 0.1, b ± 0.2.

In the case of the H^{15} azomethine protons, all three components of the larger hyperfine values were easily visible in the ^{1}H ENDOR spectra. Unfortunately, in the case of the H-bonded oxime proton (H^{16}), only two components of the hyperfine coupling are clearly visible in the experimental ENDOR spectra (effectively the experimental equivalents of A_1 and A_3, labelled * in Figure 2 and ESI 2). The third component of this tensor is buried under the inner peaks in the ENDOR spectra, originating from hyperfine couplings to the more remote protons. The reported principal values of the hyperfine tensor for H^{16} in [Cu($\mathbf{L^1}$)$_2$] are given in Table 2 with a_{iso} = -0.08 MHz and Cu…H^{16} = 2.94 Å. Using this hyperfine tensor as a starting point, the ENDOR simulations were undertaken and the resulting optimized values of the H^{16} hyperfine tensors for in [Cu($\mathbf{L^2}$)$_2$] and [Cu($\mathbf{L^3}$)$_2$] are listed in Table 2. The error associated with the A_2 value in both

cases is obviously higher compared to the clearly resolved A_1 and A_3 components. Nevertheless, some important insights into the perturbation to this H-bonded oxime proton can be obtained using these experimental hyperfine values.

Analysis of the hyperfine tensor gives a_{iso} = -0.07 MHz with $A_{\|}$ = 6.97 MHz, and these values are found to be similar to those of the related [Cu($\mathbf{L^1}$)$_2$] complex (see Table 2). By comparison, slightly different values of a_{iso} = 0.55 MHz and $A_{\|}$ = 3.65 MHz, were obtained for the [Cu($\mathbf{L^3}$)$_2$] complex. It should be noted that in our simulations the unresolved A_2 component of the H^{16} hyperfine coupling was assigned a value of -1.25 MHz for both complexes (as a peak appears at this resonance frequency in the spectra). Although the remote H^{11} protons in [Cu($\mathbf{L^1}$)$_2$] (see Scheme 2) have a reported ^{H}A tensor of [-1.26, 1.78, -1.89 MHz], and this should also be visible in [Cu($\mathbf{L^2}$)$_2$] (Figure 2), this proton is absent in [Cu($\mathbf{L^3}$)$_2$] (where it is replaced by the -N(C_6H_{13})$_2$ group) but a resonance peak is still visible at *ca*. 1.25 MHz in the spectrum, adding confidence to our assignments from the simulations for H^{16}.

The larger a_{iso} value for [Cu($\mathbf{L^3}$)$_2$] indicates a higher unpaired spin density on this H^{16} proton, whilst the smaller dipolar $A_{\|}$ value indicates a longer Cu…H^{16} distance of 3.01 Å compared to 2.92 Å in [Cu($\mathbf{L^2}$)$_2$]. These results can be explained in terms of the influence of the -N(C_6H_{13})$_2$ group in the complex, causing an asymmetric polarization of the unpaired spin density in the Cu(II) orbitals (manifested in the smaller $^{Cu}A_{\|}$ value of 620 MHz and larger a_{iso} value for H^{16}) and a lengthening of the Cu…H^{16} distance. In other words, the unpaired Cu(II) spin density appears to be polarized towards the H^{16} proton (higher a_{iso}) and away from the H^{15} proton (lower a_{iso}) due to the -N(C_6H_{13})$_2$ group in [Cu($\mathbf{L^3}$)$_2$]. Although a larger spin density occurs on H^{16} in [Cu($\mathbf{L^3}$)$_2$], the longer Cu…H^{16} distance suggests a weaker H-bond between this oxime proton (H^{16}) and the neighboring ligand phenolate oxygen.

Q-band ^{14}N ENDOR

Further information on the distribution of electron spin density in the copper complexes can be obtained from the ^{14}N ENDOR spectra. The Q-band ^{14}N ENDOR spectra for [Cu($\mathbf{L}^{2}$)$_2$] and [Cu($\mathbf{L}^{3}$)$_2$] are shown in Figure 3 and ESI 3. The ^{14}N hyperfine and quadrupole parameters were obtained by simulation of the angular selective ENDOR spectra and the resulting values are listed in Table 3. The ^{14}N hyperfine tensor is nearly axially symmetric. It has been reported that the largest principal axis is oriented approximately along the Cu-N bond direction in the [Cu($\mathbf{L}^{1}$)$_2$] single crystal[18,19] and a structurally related [Cu(msal)$_2$] complex (msal = *N*-methyl-salicylideneiminate),[29] so we can assume a similar orientation occurs in [Cu($\mathbf{L}^{2}$)$_2$] owing to the similarity in the ^{N}A and ^{N}Q values (Table 3).

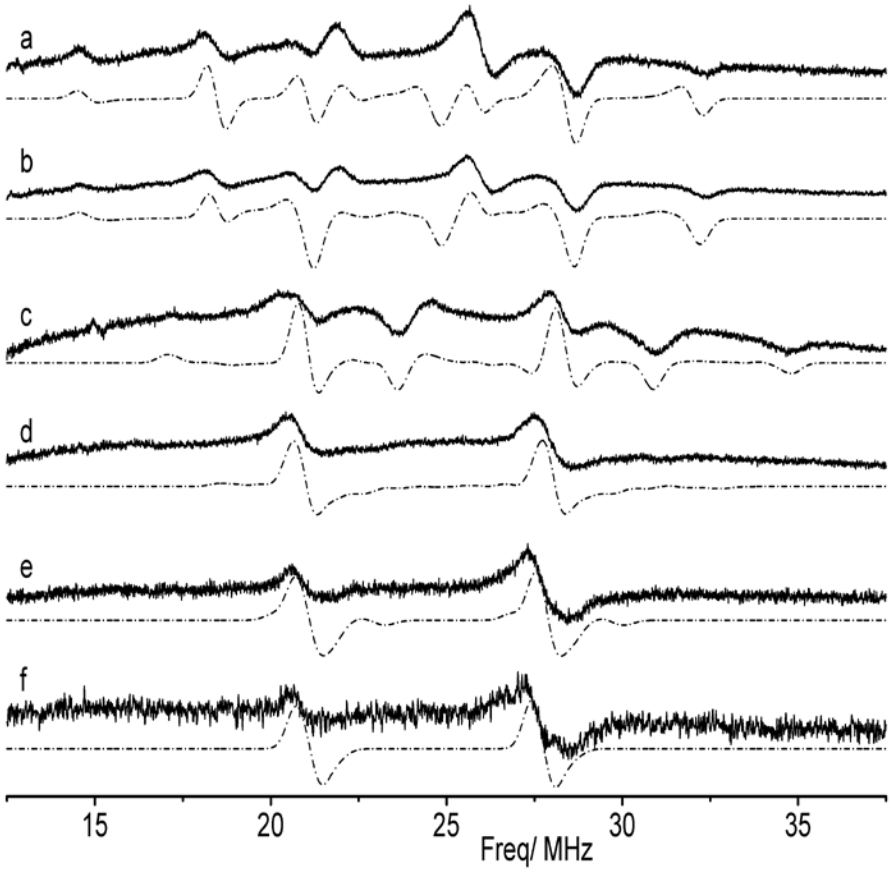

Figure 3: CW Q-band ^{14}N ENDOR spectra (10 K) for [Cu($\mathbf{L^2}$)$_2$] recorded at the field positions a) 1200.1, b) 1195.5, c) 1181.8, d) 1144.1, e) 1102.9 and (f) 1082.4 mT. Corresponding simulations are shown at each field position with dotted lines.

The hyperfine and quadrupole values for [Cu($\mathbf{L^3}$)$_2$] are also listed in Table 3. Whilst the hyperfine values ($^N A$) are similar compared to [Cu($\mathbf{L^2}$)$_2$], significant changes are observed in the quadrupole values ($^N Q$). This results in lower e^2qQ/h and asymmetry (η) parameters (Table 3). The quadrupole parameter is very sensitive to changes in electron spin density in the plane of the Cu(II) complex as variation occurs in the electric field gradient. So, in principle, subtle changes in spin redistribution in the $d_{x^2-y^2}$ orbital caused by changes from the -N(C_6H_{13})$_2$ functionality can be monitored. The changes to $^N Q$, particularly with the largest value changing from Q_2 in [Cu($\mathbf{L^2}$)$_2$] to Q_1 in [Cu($\mathbf{L^3}$)$_2$] can be accounted for by the changes in spin polarization and further supports the observed trends found earlier *via* the ^{1}H ENDOR data.

Table 3; ^{14}N hyperfine and quadrupole coupling parameters for [Cu($\mathbf{L^1}$)$_2$], [Cu($\mathbf{L^2}$)$_2$] and [Cu($\mathbf{L^3}$)$_2$].

Solvent	$^a A_1$	A_2	A_3	$^b Q_1$	Q_2	Q_3	e^2qQ/h	η
[Cu($\mathbf{L^1}$)$_2$]$_{sc}$	51.96	42.10	43.64	-1.71	1.91	-0.20	3.82	0.79
[Cu($\mathbf{L^2}$)$_2$]$_{ply}$	53.4	40.4	43.7	-1.2	1.37	-0.17	2.74	0.82
[Cu($\mathbf{L^3}$)$_2$]$_{ply}$	53.0	39.8	44.1	1.1	-0.92	-0.2	1.84	0.67

sc = Single crystal data; ply = polycrystalline toluene/dichloromethane frozen solution; All hyperfine and quadrupole values reported in MHz. $^a A$ values ± 0.2 MHz, $^b Q$ values ± 0.1 MHz.

DFT & X-ray structure

The above ENDOR data suggests that incorporation of an aminomethyl group *ortho* to the phenolic oxygen atom causes the length and therefore strength of the oxime to phenolate hydrogen bond to change significantly (evidenced by changes in Cu…^{1}H distances). The extent to which these changes in outer coordination sphere influences the structure and bonding in the inner sphere, and thus the strength of the ligands as copper extractants, is of considerable interest. To understand the origins of these substituent effects, we investigated the structure of the complexes by hybrid DFT calculations and X-ray crystallography. To reduce the numbers of possible conformers, the hybrid DFT calculations were performed on model complexes [Cu($\mathbf{L}^{4}$)$_2$] and [Cu($\mathbf{L}^{5}$)$_2$] which have methyl groups replacing the *t*-butyl and *n*-hexyl groups in [Cu($\mathbf{L}^{2}$)$_2$] and [Cu($\mathbf{L}^{3}$)$_2$]. The energy-minimized structure of [Cu($\mathbf{L}^{5}$)$_2$] has the two aminomethyl groups displaced to the same side of the coordination plane (Figure 4). A more nearly centrosymmetric form with aminomethyl groups on opposite sides of the CuN_2O_2 plane has a slightly higher energy (4.1 kJ mol^{-1}), but contains a similar arrangement of the H-bonds formed by the oximic hydrogen atoms (H^{16}).

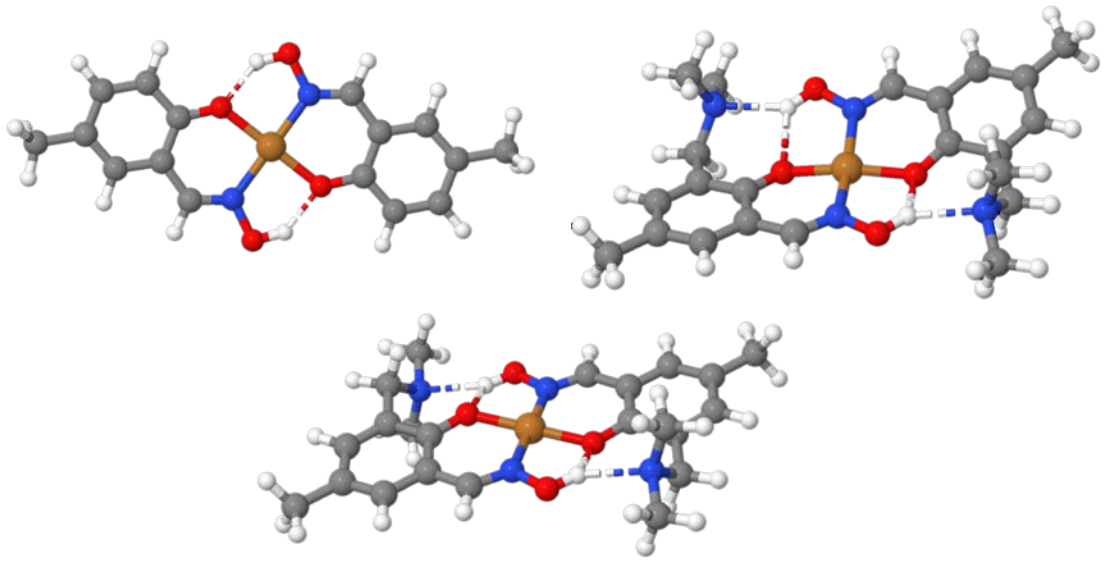

Figure 4: The energy-minimized structures of [Cu($\mathbf{L^4}$)$_2$] and [Cu($\mathbf{L^5}$)$_2$] (*top*), showing contacts made by the oximic hydrogen atoms. The slightly higher energy, centrosymmetric form of [Cu($\mathbf{L^5}$)$_2$] (*bottom*) is included for comparison.

The changes in positions of the hydrogen atoms in the aminomethyl-substituted and unsubstituted compounds [Cu($\mathbf{L^5}$)$_2$] and [Cu($\mathbf{L^4}$)$_2$] mirror those found in the ENDOR studies of [Cu($\mathbf{L^3}$)$_2$] and [Cu($\mathbf{L^2}$)$_2$]. In particular, the interaction of the H^{16} atom with the amine nitrogen atom causes it to move away from the central copper atom (see Table 4; increased Cu…H distance). This movement is accompanied by a shortening of the Cu-O bonds and a lengthening of the Cu-N bonds and, as a consequence, the azomethine hydrogen atom H^{15} becomes more remote from the copper atom, as revealed by the ENDOR spectra.

Table 4. Interatomic distances (Å) from ENDOR measurements, hybrid DFT calculations and single crystal X-ray structure determinations.

	Cu…H^{15}	Cu…H^{16}	Cu-O	Cu-N
ENDOR/ Å				
[Cu($\mathbf{L^2}$)$_2$]	3.97	2.92	-	-
[Cu($\mathbf{L^3}$)$_2$]	4.13	3.01	-	-
Hybrid DFT/ Å				
[Cu($\mathbf{L^4}$)$_2$]	3.92	2.60	1.93	1.96
[Cu($\mathbf{L^5}$)$_2$]	3.94	2.96	1.89	2.00
XRD/ Å				

[Cu($\mathbf{L^2}$)$_2$]	3.77[a,c]	2.71[a,c]	1.904(2)[a]	1.943(2)[a]
[Cu($\mathbf{L^6}$)$_2$]	3.77[b,c]	2.83[b,c]	1.896(1)[b]	1.958(2)[b]

[a]Average of three crystallographically independent values.[9] [b]Average of two crystallographically independent values present in metal complex dimer [Cu($\mathbf{L^6}$)$_2$]$_2$ (see Figure 5).[12] [c]No esd values for positional parameters are provided for H-atoms in these structures[9,11]

The strengths of the H-bonds in [Cu($\mathbf{L^4}$)$_2$] and [Cu($\mathbf{L^5}$)$_2$] were also compared using Natural Bond Order (NBO) calculations. The bond between the oximic hydrogen and the phenolate oxygen atoms in the unsubstituted compound [Cu($\mathbf{L^4}$)$_2$] is considerably stronger (39 kJ/mol) compared to [Cu($\mathbf{L^5}$)$_2$] (19 kJ/mol) (see ESI 4,5), presumably because the amine group in the latter is competing for the H-bond donor (22 kJ/mol).

The effects of an aminomethyl group substitution in the 3-position on the structures of complexes in the solid state were evaluated by comparing the single crystal X-ray structures of [Cu($\mathbf{L^2}$)$_2$][9] and [Cu($\mathbf{L^6}$)$_2$][12] (see Figure 5). The aminomethyl group in the latter complex contains a relatively rigid piperidine unit which facilitated the isolation of good quality single crystals.[11] The distortion of the CuN_2O_2 coordination geometry from planarity in [Cu($\mathbf{L^6}$)$_2$] is similar to that observed in the calculated structure of [Cu($\mathbf{L^5}$)$_2$] (Figure 4), and is enhanced by the formation of copper complex dimers, formed through one phenolate oxygen atom and the Cu atom in a neighbouring complex (Figure 5, right). Similar to the DFT structures, the Cu-N bonds are longer in the amine-substituted complex (1.958(2) *cf.* 1.943(3) Å, see Table 4), and this likely explains the observed differences in the ^{N}A and ^{N}Q values observed by ENDOR. The differences between the averaged Cu-O lengths follow the variations predicted by the DFT calculations but are barely statistically significant, possibly as a consequence of the phenolate groups in each solid state structure having different environments. In each structure, one phenolate oxygen atom

forms a weak bond to a copper atom in an adjacent complex, forming a dimer in the case of [Cu($\mathbf{L}^{6}$)$_2$] and a more extended array in [Cu($\mathbf{L}^{2}$)$_2$] (see Figure 5).

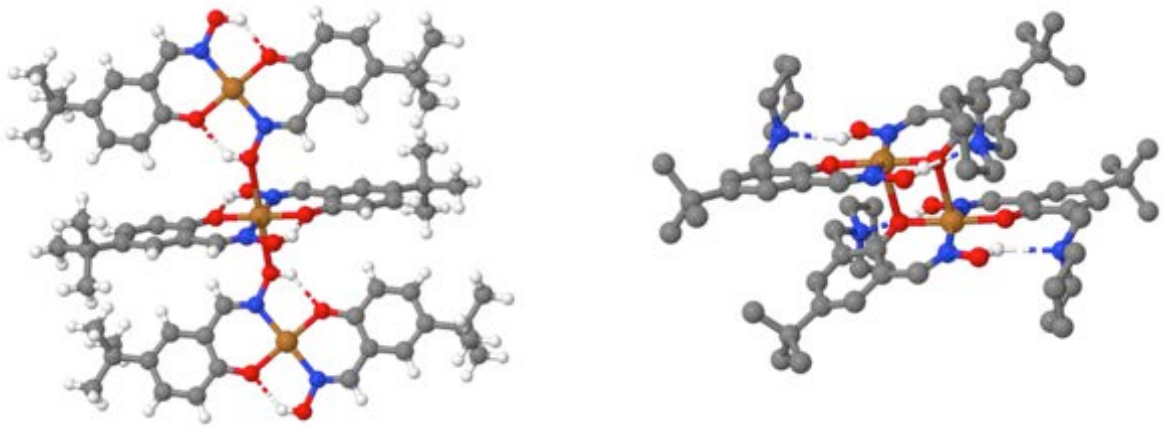

Figure 5: Part of the X-ray crystal structure of [Cu($\mathbf{L}^{2}$)$_2$] and a view of the [Cu($\mathbf{L}^{6}$)$_2$]$_2$ dimer. For clarity, hydrogen atoms attached to carbon have been omitted from the latter.

Using the X-ray crystal structures of [Cu($\mathbf{L}^{2}$)$_2$] and [Cu($\mathbf{L}^{6}$)$_2$] to follow the effects of substitution on differences in the positions of the oximic hydrogen (H^{16}) atoms is difficult because the published structure have these atoms in calculated positions riding on their attached oxygen atoms. Consequently the apparent lengthening of the Cu…H^{16} distance in the buttressed complex [Cu($\mathbf{L}^{6}$)$_2$] associated with H^{16} being "pulled" towards the amine group (Table 4) is not statistically significant. However, it is possible to track the movement of the oximic *oxygen* atom away from the copper towards the aminomethyl group in [Cu($\mathbf{L}^{6}$)$_2$] (see ESI 4). The mean Cu…O_{oxime} distance in [Cu($\mathbf{L}^{6}$)$_2$] is 2.923(2) *c.f.* 2.855(2) Å in [Cu($\mathbf{L}^{2}$)$_2$] which is consistent with results from the ENDOR and DFT studies above.

As mentioned above, the incorporation of substituents *ortho* to the phenol group has been shown to have a major effect on the strength as Cu-extractants in the pH-dependent equilibrium.[9] Copper extractions by chloroform solutions of $\mathbf{L}^{2}$H and $\mathbf{L}^{3}$H are presented in Figure 6 and

compared with the strongest of a series of salicylaldoxime extractants (the 3-bromo-substituted $\mathbf{L}^{9}$H) and the weakest (the 3-*t*-butyl-substituted $\mathbf{L}^{10}$H). The 3-aminomethyl-substituted extractant $\mathbf{L}^{3}$H is only slightly stronger than the unsubstituted reagent, $\mathbf{L}^{2}$H, having a $pH_{0.5}$ value (the pH for 50% metal-loading) of 1.45. At first sight this is surprising, given the very strong "buttressing" of intramolecular H-bonding, which has been demonstrated above, and the observation that such buttressing is the dominant factor in determining the relative strengths of the eight extractants studied previously.[9] The anomalous behavior of the 3-aminomethyl substituent in $\mathbf{L}^{3}$H can be understood by using hybrid DFT calculations to compare substituent effects on the deprotonation energies of the proligands ($\Delta U_{dp,}$ eq.1), the binding energies of the anionic ligands to Cu^{2+} (ΔU_b, eq.2) and the formation energies of the copper complexes (eq.3, $\Delta U_f = \Delta U_{dp} + \Delta U_b$).

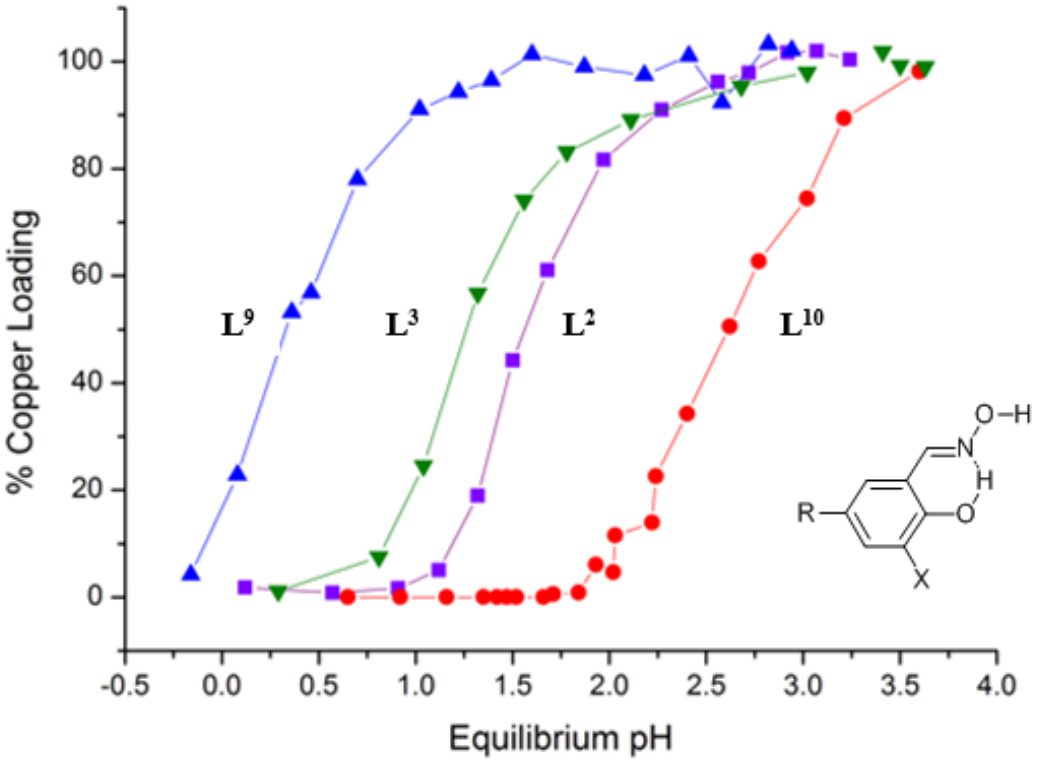

Figure 6: The pH profiles for copper extraction by 0.01 M chloroform solutions of $\mathbf{L}^{2}$H, $\mathbf{L}^{3}$H, $\mathbf{L}^{9}$H and $\mathbf{L}^{10}$H from equal volumes of 0.01 M aqueous solutions of $CuSO_4$; 100% loading represents Cu-uptake corresponding to formation of a 1:2 complex Cu$\mathbf{L}_2$.

$$(\mathbf{L}H)_2 \rightleftharpoons 2\mathbf{L}^- + 2H^+ \quad (1)$$

$$Cu^{2+} + \mathbf{L}^- \rightleftharpoons [Cu(\mathbf{L})_2] \quad (2)$$

$$Cu^{2+} + (\mathbf{L}H)_2 \rightleftharpoons [Cu(\mathbf{L})_2] + 2H^+ \quad (3)$$

Table 5: Calculated dimerization (eq. 4), deprotonation (eq. 2), binding (eq. 3) and complex formation energies (eq.1).

LH		ΔU_{dim} /kJ mol^{-1}	ΔU_{dp} /kJ mol^{-1}	ΔU_b /kJ mol^{-1}	ΔU_f /kJ mol^{-1}
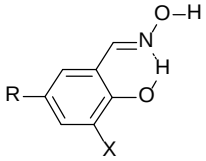	X				
$\mathbf{L}^{4}$H	H	-40.4	3031.0	-2897.2	133.8
$\mathbf{L}^{5}$H	$CH_2N(CH_3)_2$	-73.4	3053.5	-2905.4	148.1
$\mathbf{L}^{7}$H	Br	-44.8	2969.5	-2843.3	126.2
$\mathbf{L}^{8}$H	^{t}Bu	-28.8	3000.8	-2830.3	170.5

The calculated formation energies of the Cu-complexes (ΔU_f, Table 5) are increasingly favorable in the order: $\mathbf{L}^{8}$H < $\mathbf{L}^{5}$H < $\mathbf{L}^{4}$H < $\mathbf{L}^{7}$H, (*i.e.*, as the X substituent is changed from *t*-Bu, to CH_2-N-morpholine, to H and to Br). The bromo-substituted reagent $\mathbf{L}^{7}$H is predicted to be the strongest extractant because it has the lowest deprotonation energy (ΔU_{dp}) and the second most favorable inter-ligand hydrogen bonding as revealed by the dimerization energies (ΔU_{dim}). The former can be ascribed to the electron withdrawing properties of the bromide and the latter is consistent with some form of additional intra-complex secondary bonding, such as buttressing of the H-bonding,[9] that contributes to the stability of the Cu complex. These terms, which favor complex-formation, more than compensate for the weaker binding energy to Cu(II) which arises from the bromo substituent reducing the basicity of the $N_2O_2^{2-}$ donor set.

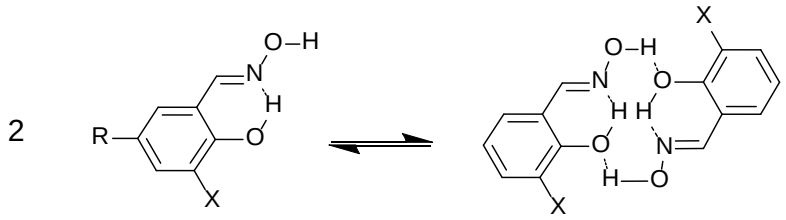

$$2H\mathbf{L} \rightleftharpoons (H\mathbf{L})_2 \qquad (4)$$

Figure 7: Dimerization to give the proligands with preorganised N_2O_2 donor sets.

The ENDOR, hybrid DFT and X-ray structural data above all indicate that the aminomethyl substituent *ortho* to the phenolic oxygen atom provides particularly strong buttressing of inter-ligand H-bonding. This is manifested by $\mathbf{L}^{5}$H having the most favorable dimerization energy (ΔU_{dim} Table 5) for the process shown in Figure 7 and eq.4. Whilst the buttressed H-bonding is very favorable in the proligand dimer [$\mathbf{L}^{5}$H]$_2$ in the gas phase, it preorganizes the N_2O_2 donor set

to give a non-planar arrangement (Figure 8) which is a poor fit for Cu(II). Consequently the binding energy to Cu(II) (ΔU_b) is smaller than in the unsubstituted reagent $\mathbf{L}^4$H and does not compensate for its high deprotonation energy.

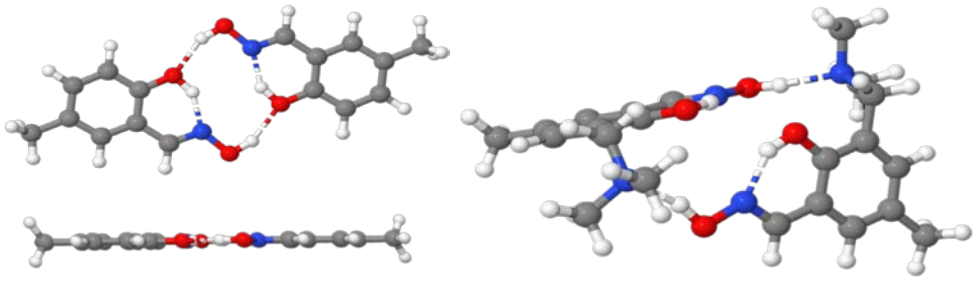

Figure 8: The energy-minimized structures of the proligand dimers $[\mathbf{L}^4H]_2$ and $[\mathbf{L}^5H]_2$, contrasting the planar preorganization of the N_2O_2 donor set in $[\mathbf{L}^4H]_2$ (left) and the non-planar arrangement in $[\mathbf{L}^5H]_2$ (right).

The combination of techniques described above has demonstrated that buttressing of H-bonding in the outer coordination sphere of extracted metal complexes significantly influences their structures and stabilities. However, the work also reveals that it will not always be the case that reagents which provide the strongest buttressing will prove to be the strongest extractants; the buttressing may impose an unfavorable coordination geometry on the complexed metal.

Conclusions

EPR and ENDOR spectroscopy at two different frequencies, used to investigate Cu(II) complexes bearing 3-X-salicylaldoximes in frozen solution, provide information for the first time on the relative strengths of hydrogen bonds formed in a medium/environment which is similar to that used in commercial solvent extraction processes. This information is important because the

selectivity and strength of copper extraction is known to be dependent on inter-ligand H-bonding.[3a]

The $\boldsymbol{g}$ and $^{Cu}\boldsymbol{A}$ spin Hamiltonian parameters extracted by simulation of the EPR spectra confirm the square planar geometry of the complexes, and the observed values were found to be in close agreement with the reported values for the unsubstituted doped single crystal of $[Cu(\mathbf{L^1})_2]$.[17] Analysis of the Q-band ^{1}H and ^{14}N ENDOR data reveal an asymmetric spin polarization of the unpaired electron caused by the peripheral $-N(C_6H_{13})_2$ groups in $[Cu(\mathbf{L^3})_2]$. This is manifest through a higher a_{iso} value for the oxime H^{16} atom and a lower a_{iso} value for the azomethine H^{15} atom compared to $[Cu(\mathbf{L^2})_2]$. Crucially the Cu…H^{16} distance was found to be noticeably longer in $[Cu(\mathbf{L^3})_2]$ than in $[Cu(\mathbf{L^2})_2]$, as determined from the dipolar component of the ^{1}H hyperfine tensor using the point dipole approximation. This can be interpreted in terms of a weaker H-bond between the oxime proton (H^{16}) and the coordinated phenolate oxygen in $[Cu(\mathbf{L^3})_2]$, resulting from polarization of the H^{16} proton towards the $-CH_2N(C_6H_{13})_2$ group. These changes in inter-ligand H-bonding, arising from the introduction of an aminomethyl group, are mirrored in the structures of closely related model complexes obtained in the gas phase by DFT calculations and in the solid state by X-ray structure determination.

Earlier work suggested that the ability of 3-X-substituents in salicylaldoximes to “buttress” the H-bonding between ligands in the outer coordination sphere is the dominant effect in determining their strength as copper extractants. In this paper the combination of structural investigations and DFT calculations of energies of formation for the copper complexes has revealed that this is not always the case. The very strong additional (buttressing) H-bonds formed by aminomethyl substituents do not greatly increase the strength of copper extraction because they impose an unfavourable geometry on the complexed metal. These substituents also increase

the energy required to deprotonate the extractant and thereby form the neutral complexes with Cu(II).

AUTHOR INFORMATION

Corresponding Authors

* Email: MurphyDM@cardiff.ac.uk. * Email: P.A.Tasker@ed.ac.uk

Author Contributions

The manuscript was written with contributions from all authors. All authors have given approval to the final version of the manuscript.

ACKNOWLEDGMENT

We thank the EPSRC and Cytec Industries for funding for PhD studentships for RSF, RJG and MRH and PDRA funding (EC), the EaStCHEM research computing facility for access to software and the Edinburgh Computer and Data Facilities (ECDF) for access to hardware.

ASSOCIATED CONTENT

Supporting Information. Q-band CW EPR spectra, X-band ^{1}H ENDOR spectra, Q-band ^{14}N ENDOR spectra of [Cu(**L**^{3})$_2$], calculated and found intramolecular Cu---O_{oxime} and O_{phenol}---O_{oxime} distances and NBO-calculated energies of H-bonds formed by the oxime H[16] in selected complexes and proligand dimers, and Cartesian coordinates for all energy minimized structures. This material is available free of charge via the Internet at http://pubs.acs.org.

REFERENCES

(1) Hamilton, J. A.; Sabesan, M. N.; Steinrauf, L. K. *J. Am. Chem. Soc.* **1981**, *103*, 5880.

(2) Godycki, L. E.; Rundle, R. E. *Acta Cryst.* **1953**, *6*, 487.

(3) a) Turkington, J. R.; Bailey, P. J.; Love, J. B.; Wilson, A. M.; Tasker, P. A. *Chem. Comm.* **2013**, *49*, 1891; b) Wilson, A.M.; Bailey, P. J.; Tasker, P.A.; Turkington, J.R.; Grant, R.A.; Love, J.B. *Chem. Soc. Rev.*, **2014**, *43*, 123

(4) a) Tasker, P. A.; Plieger, P. G.; West, L. C. *Comprehensive Coordination Chemistry II* **2004**, *9*, 759. b) Nicol, M. J.; Fleming, C. A.; Preston, J. S. *Comprehensive Coordination Chemistry* **1987**, *6*, 779.

(5) a) Brammer, L Dalton Trans. 2003, 3145. b) Belkova, N.V.; Shubina, E.S.; Epstein, L.M. Acc. Chem. Res. 2005, 38, 624. c) Grabowski, S.J.; Chem Rev 2011, 111, 2597.

(6) a) Cole, P. M.; Sole, K. C.; Feather, A. M. *Tsinghua Sci. Tech.* **2006**, *11*, 153; b) Sole, K. C.; Feather, A. M.; Cole, P. M. *Hydrometallurgy* **2005**, *78*, 52.

(7) Szymanowski, J. *Hydroxyoximes and Copper Hydrometallurgy*, CRC Press, Boca Raton, USA, **1993.**

(8) a) Mackey, P. J. in *CIM Magazine, Vol. 2*, **2007**, 35; b) Kordosky, G. A. *International Solvent Extraction Conference, Cape Town, South Africa, Mar. 17-21* **2002**, 853.

(9) Forgan, R. S.; Roach, B. D.; Wood, P. A.; White, F. J.; Campbell, J.; Henderson, D. K.; Kamenetzky, E.; McAllister, F. E.; Parsons, S.; Pidcock, E.; Richardson, P.; Swart, R. M; Tasker, P. A. *Inorg. Chem.* **2011**, *50*, 4515.

(10) Smith, A. G.; Tasker, P. A.; White, D. J. *Coord. Chem. Rev.* **2003**, *241*, 61.

(11) Forgan, R. S.; Davidson, J. E.; Fabbiani, F. P. A.; Galbraith, S. G.; Henderson, D. K.; Moggach, S. A.; Parsons, S.; Tasker, P. A.; White, F. J. *Dalton Trans.* **2010**, *39*, 1763.

(12) Stoll, S.; Schweiger, A. *J. Magn. Reson.* **2006,** *178*, 42.

(13) Gaussian 09, Revision D.01, Frisch, M. J.; Trucks, G. W.; Schlegel, H. B.; Scuseria, G. E.; Robb, M. A.; Cheeseman, J. R.; Scalmani, G.; Barone, V.; Mennucci, B.; Petersson, G. A.; Nakatsuji, H.; Caricato, M.; Li, X.; Hratchian, H. P.; Izmaylov, A. F.; Bloino, J.; Zheng, G.; Sonnenberg, J. L.; Hada, M.; Ehara, M.; Toyota, K.; Fukuda, R.; Hasegawa, J.; Ishida, M.; Nakajima, T.; Honda, Y.; Kitao, O.; Nakai, N.; Vreven, T.; Montgomery, J. A.; Peralta, J. E.; Ogliaro, F.; Bearpark, M.; Heyd, J. J.; Brothers, E.; Kudin, K. N.; Staroverov, V. N.; Kobayashi, R.; Normand, J.; Raghavachari, K.; Rendell, A.; Burant, J. C.; Iyengar, S. S.; Tomasi, J.; Cossi, M.; Rega, N.; Millam, J. M.; Klene, M.; Knox, J. E.; Cross, J. B.; Bakken, V.; Adamo, C.; Jaramillo, J.; Gomperts, R.; Stratmann, R. E.; Yazyev, O.; Austin, A. J.; Cammi, R.; Pomelli, C.; Ochterski, J. W.; Martin, R. L.; Morokuma, K.; Zakrzewski, V. G.; Voth, G. A.; Salvador, P.; Dannenberg, J. J.; Dapprich, S.; Daniels, A. D.; Farkas, Ö.; Foresman, J. B.; Ortiz, J. V.; Cioslowski, J.; Fox, D. J. *Gaussian, Inc.*, Wallingford CT, **2009**.

(14) Glendening, D.; Badenhoop, J. K.; Reed, A. E.; Carpenter, J. E.; Bohmann, J. A.; Morales, C. M.; Weinhold, F. *NBO 5.G*. Theoretical Chemistry Institute, University of Wisconsin, Madison, WI, **2001**.

(15) (a) Becke, A. D. *J. Chem. Phys.* **1993**, *98*, 5648. (b) Lee, C.; Yang, W.; Parr, R. G. *Phys. Rev. B: Condens. Matter* **1988**, 37, 785.

(16) Boys, S. F.; Bernardi, F. *Mol. Phys.* **1970**, *19*, 553.

(17) Schweiger, A.: *Struct. Bonding (Berlin),* **1982**, *51*, 1.

(18) Schweiger, A.; Gunthard, Hs.H. *Chem. Phys.* **1978**, *32*, 35.

(19) Schweiger, A.; Rist, G.; Gunthard, Hs.H. *Chem. Phys. Lett.* **1975**, *31*, 48.

(20) a) McCudden, B.; O'Brien, P.; Thornback, J. R. *Dalton Trans.* **1983**, 2043. b) O'Brien, P.; Thornback, J. R.; Szymamowski, J. *J. Coord. Chem.* **1983**, *13***,** 11.

(21) Ovchinikov, I. V., Konstantinov, V. N., *J. Mag. Reson*. **1978**, *32*, 179.

(22) Mabbs, F. E., Collison, D. Studies in Inorganic Chemistry 16: *Electron Paramagnetic Resonance of d-Transition Metal Compounds,* Elsevier, **1992**.

(23) Pilbrow, J. R.; *Transition Ion Electron Paramagnetic Resonance*, Oxford Science Publications, Oxford, **1990**.

(24) Rist, G. H.; Hyde, J. S. *J. Chem. Phys*. **1970**, *52*, 4633.

(25) a) Hoffman, B. M.; Martinsen, J.; Venters, J. *J. Magn. Reson*. **1984**, *59*, 110. b) Hoffman, B. M.; Venters, J.; Martinsen, J. *J. Magn. Reson*. **1985**, *62*, 537.

(26) a) Hurst, G. C.; Henderson, T. A.; Kreilick, R. W. *J. Am. Chem. Soc*. **1985**, *107*, 7294. b) Henderson, T. A.; Hurst, G. C.; Kreilick, R. W. *J. Am. Chem. Soc*. **1985**, *107*, 7299.

(27) Murphy, D. M.; Farley, R. D. *Chem. Soc. Rev*. **2006**, *35*, 249.

(28) Attanasio, D. *J. Phys. Chem*. **1986**, *90*, 4952.

(29) Moores, B. W.; Belford, R. L. *Electron Spin Resonance of Metal Complexes*, Yen, T.F.; ed., New York, Plenum Press, **1969**, 13.

Graphical Abstract

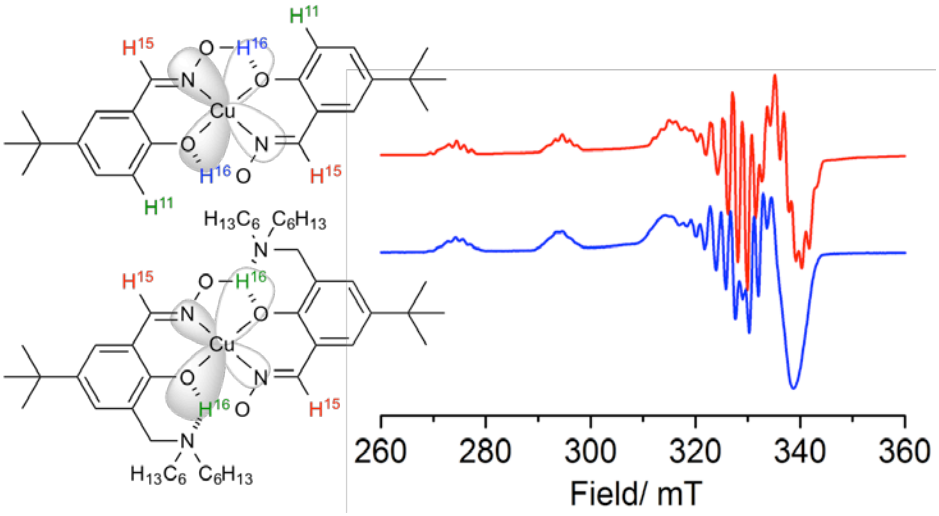

EPR, ENDOR, DFT and X-ray crystallography were collectively used to characterize a series of Cu(II) complexes of phenolic oximes of relevance as copper extractants. Evidence of outer sphere substituents 'buttressing' the inter-ligand H-bonding (between the oximic proton and phenolate oxygen) in these complexes for enhancement in extractant strength, is presented.